

# High-temperature powder synchrotron diffraction studies of synthetic cryolite $\text{Na}_3\text{AlF}_6$

Qingdi Zhou and Brendan J. Kennedy\*

*School of Chemistry, The Centre for Heavy Metals Research, The University of Sydney, Sydney 20006, Australia*

Received 3 June 2003; received in revised form 28 July 2003; accepted 6 August 2003

## Abstract

A high-resolution synchrotron diffraction study of the structures of a synthetic sample of cryolite  $\text{Na}_3\text{AlF}_6$  from room temperature to  $800^\circ\text{C}$  is reported. At room temperature  $\text{Na}_3\text{AlF}_6$  is monoclinic and the structure is described in space group  $P2_1/n$ . Heating the sample to  $560^\circ\text{C}$  results in only minor changes to the structure. A first-order transition from this monoclinic structure to a high-temperature cubic structure is observed near  $567^\circ\text{C}$ . The cubic  $Fm\bar{3}m$  structure is characterized by disorder of the fluoride atoms.

Crown Copyright © 2003 Published by Elsevier Inc. All rights reserved.

*Keywords:* Perovskite; Cryolite; Phase transition

## 1. Introduction

Compounds whose structures are based on the  $\text{ABX}_3$  perovskite motif are of considerable interest over a wide range of scientific and technical fields. The vast majority of interest has been focused on the oxide perovskites as a consequence of the array of electronic and magnetic properties displayed by these oxides [1,2]. In comparison the fluoride perovskites, most of which have a double perovskite ( $\text{A}_2\text{BB}'\text{X}_6$ ) type structure and are isostructural with elpasolite,  $\text{K}_2\text{NaAlF}_6$ , have historically been of interest mainly as hosts in spectroscopic studies of various lanthanide ions. Such studies have revealed the halide containing perovskites display an array of structural phase transitions [3].

The cubic elpasolite structure is on a double perovskite cell  $a_e \approx 2a_p$ , where  $a_e$  and  $a_p$  are the cubic cell parameters of elpasolite and perovskite. In the cubic double perovskite or elpasolite structure all the cations lie on special positions. The  $\text{Al}^{3+}$  ions occupy a face-centered cubic (fcc) lattice and each ion is octahedrally surrounded by six  $\text{F}^-$  ions located at a distance  $\pm x$  along the three four-fold crystal axes. The  $\text{Na}^+$  ions occupy similar octahedral sites and together they form a

simple cubic lattice. The  $\text{AlF}_6$  and  $\text{NaF}_6$  octahedra are corner connected in three dimensions (see Fig. 1). The  $\text{K}^+$  ions are surrounded by 12  $\text{F}^-$  ions. The Al–F and Na–F distances are then given by the lattice parameter and the value of  $x$ . The cell doubling observed in elpasolite is a result of a rock-salt like ordering of the two different B-type cations, Fig. 1. The ordering of the two B-type cations, Al and Na, arises from differences in their size and bonding properties.

In the  $\text{ABX}_3$  perovskites changes in the ratio of the sizes of the A and B type cations may result in tilting or rotations of the  $\text{BX}_6$  octahedra, lowering their symmetry from cubic [4]. Indeed the mineral perovskite ( $\text{CaTiO}_3$ ) is actually orthorhombic space group  $Pnma$  [5] as is neighborite,  $\text{NaMgF}_3$  [6]. Similar tilts occur in the double perovskites. For example elpasolite is cubic at room temperature but replacing the two K cations with Na to give cryolite,  $\text{Na}_3\text{AlF}_6$ , results in a lowering of symmetry to monoclinic [3]. Increasing the temperature inevitably results in a reduction of the tilting of the  $\text{BX}_6$  octahedra in the  $\text{ABX}_3$  perovskites [5]. In numerous cases this leads to structural transitions to higher symmetry structures (5, 7–10). Similar events occur for the double perovskites [3]. In their early work Steward and Rooksby [11] showed cryolite undergoes a phase transition near  $550^\circ\text{C}$ ; they concluded the structure of the high-temperature form was cubic and it was

\*Corresponding author. Fax: +61-2-9351-3329.

E-mail address: [b.kennedy@chem.usyd.edu.au](mailto:b.kennedy@chem.usyd.edu.au) (B.J. Kennedy).

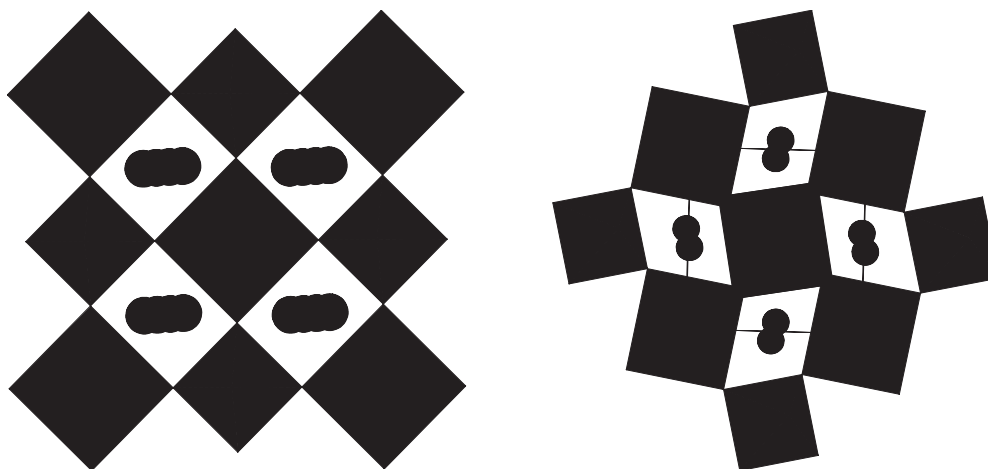


Fig. 1. Representation of the structure of cryolite,  $\text{Na}_3\text{AlF}_6$  in both the high-temperature cubic and low-temperature monoclinic forms. The smaller hatched octahedra are the  $\text{AlF}_6$  octahedra and the unshaded octahedra the larger  $\text{NaF}_6$  groups. The perovskite A-type Na cations are represented by the spheres.

isostructural with elpasolite. Yang and co-workers [12] however suggested the high-temperature structure is in fact orthorhombic in space group  $Immm$ .

The current paper describes high-resolution synchrotron diffraction studies of a synthetic sample of  $\text{Na}_3\text{AlF}_6$ , with particular emphasis on the high-temperature phase transition. We find, in agreement with the early work of Steward and Rooksby [11] and in contrast to that of Yang et al. [12], that the high-temperature phase is cubic. We observe unusual cation disorder in the high-temperature cubic phase.

## 2. Experimental

Room temperature and variable temperature (100–800°C) synchrotron X-ray diffraction patterns were recorded on the Debye–Scherrer diffractometer at beamline 20B, the Photon Factory Japan [13]. The synthetic sample (Aldrich) was finely ground and housed in a 0.3 mm dia quartz capillary for the measurements. Data were collected over the angle range  $5 \leq 2\theta \leq 70^\circ$  using two image plates as the detector with an incident wavelength of  $\lambda = 0.75 \text{ \AA}$ . Data were collected in two stages, firstly from 100 to 800°C in 25° steps. Then a second sample was investigated from 500 to 600°C in 5° steps.

### 2.1. Structural analysis

Structures were refined using the Rietveld method implemented in the program Rietica [14] where the instrumental parameters were refined using a Pseudo-Voigt profile shape function. The background was estimated by interpolation of up to 40 points. A number of weak peaks were observed due to scatter from the

furnace and the regions in the diffraction patterns affected by such peaks were excluded in the refinements.

## 3. Results and discussion

### 3.1. Room temperature structure

The refinement of the structure of  $\text{Na}_3\text{AlF}_6$  at room temperature was performed in space group  $P2_1/n$  using the structural parameters reported by Hawthorne and Ferguson [15] as a starting model. In Glazers [16] notation the structure has an  $a^-b^-c^+$  tilt pattern. The in-phase or tilts give rise to R-point reflections whereas the out-of-phase (+) tilts give rise to M-point reflections. The ordering of the Na and Al cations also gives rise to R-point reflections in the diffraction pattern. The appropriateness of this space group was confirmed by the appearance of both R- and M-point reflections, together with the obvious monoclinic splitting of the appropriate Bragg reflections in the diffraction patterns. The refinement was straightforward and the refined structural parameters and bond distances are in excellent agreement with those obtained by in the early study of Hawthorne and Ferguson [15] from a single crystal of a natural cryolite sample, Table 1, as well as in the later studies of Yang et al. [12] and Ross et al. [17]. The very small differences between these various studies possibly arises from the presence of various other trace elements in the natural cryolite samples used. The rotations of the  $\text{MF}_6$  octahedra result in  $\text{Na}_3\text{AlF}_6$  having a  $\sqrt{2}a \times \sqrt{2}b \times 2c$  superstructure relative to that of the prototype  $\text{ABX}_3$  perovskite cell.

As an aside  $\text{Na}_3\text{AlF}_6$  is an interesting compound for diffraction studies since the three ions are all isoelectronic. Whilst the identity of the atoms at the various sites cannot be confirmed the refined bond distances

make chemical sense and thus vindicate the choice of the locations of the Na and Al atoms in the two B-type positions. The difference in size and charge of the two cations results in ordering of these. Clearly it is not possible to comment on the possibility of incomplete ordering of the Na and Al cations. It is possible that the extent of ordering in our synthetic sample is different to that found in the various naturally occurring cryolite samples.

### 3.2. High-temperature structure

The synchrotron diffraction patterns recorded at or above 570°C could all be indexed on the basis of a primitive cubic cell with  $a \approx 7.93 \text{ \AA}$ . A LeBail type analysis of the profiles assuming space group  $Fm\bar{3}m$  satisfactorily accounted for all the observed Bragg reflections and it was concluded that the cubic phase has an undistorted elpasolite, double perovskite, structure in which the rock-salt type ordering of the Na and Al cations persists. Attempts to refine the structure in this model resulted in unusually poor fits to the observed data and the displacement parameters for the F atoms were anomalously high. The other structural parameters appeared reasonable although surprisingly the displacement parameters for the Al reduced from  $2.0(1) \text{ \AA}^3$  at 550°C to  $0.6(1) \text{ \AA}^3$  at 600°C. The orthorhombic  $Immm$  model proposed by Yang et al. [12] was also unsatisfactory and in this case the refined lattice parameters always indicated the structure to be metrically cubic.

Examination of the diffraction patterns demonstrated the calculated intensity, in  $Fm\bar{3}m$ , of some peaks to be

systematically underestimated, whereas others were overestimated. A Fourier difference map showed extra off-center scattering density around the F site indicating static displacive disorder. Attempts to model this using anisotropic displacement parameters for the F atoms were unsuccessful, and so a model in which the fluorides were disordered away from the 24e sites was sought. A number of models in which disorder of the fluoride atoms was allowed were then considered together with the possibilities of both cation and anion vacancies. The best fit was obtained when the F anions were allowed to move from the 24e sites at  $00z$ ,  $z \approx 0.28$  to a nearby 96k site at  $(x\ x\ z)$   $x \approx 0$   $z \approx 0.28$  but with an occupancy of 25%. This resulted in a dramatic improvement in the quality of the fit as seen both by the R-factors, Table 2 and by visual examination of the profiles, Fig. 2. The inclusion of either cation or anion vacancies did not significantly improve the quality of fit and it was concluded that  $\text{Na}_3\text{AlF}_6$  retains its composition at the temperatures studied. This model is displayed in Fig. 3.

The static disorder of the F anions is apparently a consequence of unfavorable bonding contacts in the cubic phase. The refined Al–F and Al–F bond distances in the monoclinic phase at 550°C are not significantly different to those observed at room temperature, Table 3. However at 600°C the refined Al–F distance becomes unreasonably small,  $1.717 \text{ \AA}$  and the Na–F distance ( $2.254 \text{ \AA}$ ) within the  $\text{NaF}_6$  octahedra is smaller than expected. Conversely the average Na–F distance for the 8-coordinate Na cations is somewhat larger than expected. The displacement of the F atoms by  $0.53 \text{ \AA}$  along the (110) direction has the effect of significantly increasing the Al–F distance whilst the Na–F distances within the  $\text{NaF}_6$  octahedra also increase. The average Na–F distance for the second Na cations in the perovskite A-type sites decreases somewhat as a result of the fluoride atoms being disordered over the 96k site, Table 3. In this regard the movement of the F anions has the same effect as tilting of the octahedra around the undersized A-type cations. We note that the earlier study of Yang et al. also revealed unusually large atomic displacement parameters in the high-temperature phase which they ascribed to “considerable temporal as well as spatial fluctuation” [12]. These apparent fluctuations are well modeled by the disordered model presented here.

Table 1  
Positional and thermal parameters for synthetic cryolite  $\text{Na}_3\text{AlF}_6$  at room temperature

Atom	Site	$x$	$y$	$z$	$B$
Al1	2a	0	0	0	1.2(1)
Na1	2b	0	0	0.5	0.8(1)
Na2	4e	0.5140(7)	0.9492(3)	0.2480(6)	1.5(1)
F1	4e	0.1043(4)	0.0471(4)	0.2197(5)	0.7(1)
F2	4e	0.7265(7)	0.1773(7)	0.0488(6)	1.1(1)
F3	4e	0.1645(6)	0.2746(7)	0.9368(5)	0.9(1)

The figures in parenthesis are the standard errors.  $R_p$  2.33,  $R_{wp}$  2.15,  $\chi^2$  3.28%.  $a = 5.3956(2)$ ,  $b = 5.5821(2)$ ,  $c = 7.7568(2)$ ,  $\text{Å}$   $\beta = 90.181(1)^\circ$ .

Table 2  
Positional and thermal parameters for synthetic cryolite at 600°C

Atom	Ordered model $R_p$ 5.0 $R_{wp}$ 6.8				Disordered Model 2 $R_p$ 3.3 $R_{wp}$ 4.3			
	Site	$x = y$	$z$	$B$	Site	$x = y$	$z$	$B$
Na	4a	0	0	4.4(3)	4a	0	0	3.7(1)
Al	4b	0.5	0.5	0.6(1)	4b	0.5	0.5	2.0(1)
Na	8c	0.25	0.25	5.5(2)	8c	0.25	0.25	6.3(1)
F	24e	0	0.2838(7)	9.2(3)	96k	0.0468(4)	0.2828(3)	2.5(2)

The differences between the ordered and disordered models are explained in the text.

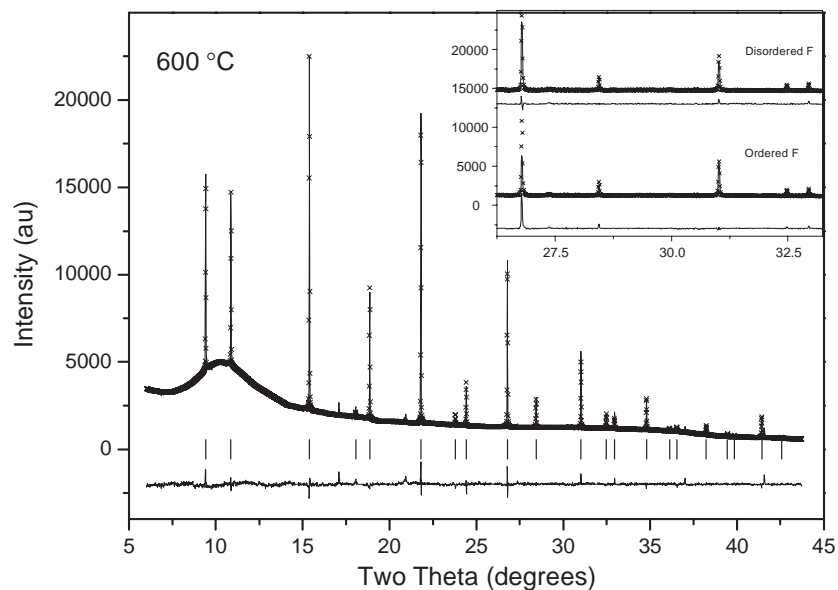


Fig. 2. Observed, calculated and difference synchrotron profiles for  $\text{Na}_3\text{AlF}_6$  at  $600^\circ\text{C}$ . The inset shows the notably better fit obtained when the F atoms are disordered on a  $96k$  site at  $x, x, z$  with  $x \approx 0$  and  $z \approx \frac{1}{4}$ .

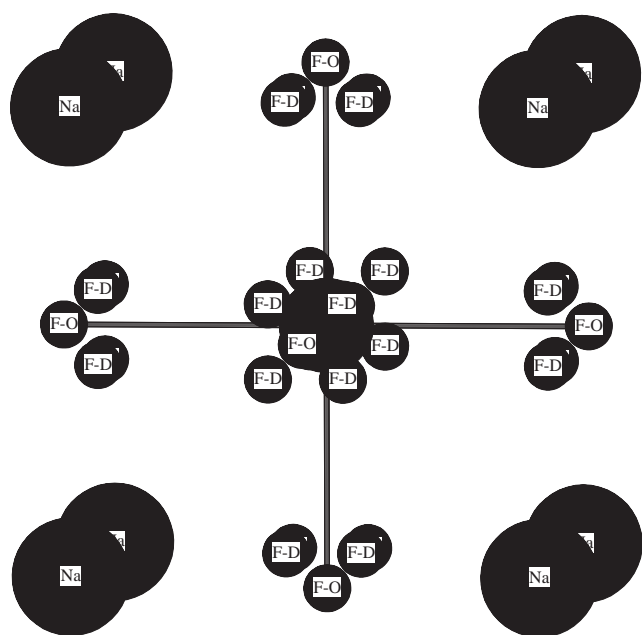


Fig. 3. Representation of the disorder of the F atoms in the high-temperature cubic phase. The F atoms in the ordered structure are at the  $24e(00z)$  site and are labeled F-O and the disordered F at the  $96k$  site are labeled F-D.

Static disorder has been observed in a number of  $\text{ABX}_3$  perovskites, most noticeably in  $\text{PbZrO}_3$  [18]. Its occurrence in double perovskites is less well known. Marx and Ibberson [19] found disorder of the Li atoms in  $\text{Li}_6\text{NBr}_3$  that has the anti-elpasolite structure (i.e. the N and one type of Br anions are at the center of the rock salt octahedra). In this case they placed the Li onto a  $96j$  site at  $x y 0$  with  $x \approx 0.25$  and  $y \approx 0$ . The  $R$ -factors do not distinguish between this model and that proposed

Table 3  
Bond distances ( $\text{\AA}$ ) for synthetic cryolite at selected temperatures

Bond	$25^\circ\text{C}$ monoclinic	$550^\circ\text{C}$ monoclinic	$600^\circ\text{C}$ cubic ordered model	$600^\circ\text{C}$ cubic disordered model
Al–F	1.768(5)	1.764(6)	1.717(6)	1.803(3)
	1.799(5)	1.782(9)		
	1.828(4)	1.801(6)		
	<b>1.798</b>	<b>1.782</b>		
Na(1)–F	2.299(4)	2.297(8)	2.254(6)	2.307(3)
	2.219(5)	2.282(6)		
	2.271(5)	2.314(7)		
	<b>2.263</b>	<b>2.298</b>		
Na(2)–F	<b>2.506</b>	<b>2.604</b>	2.820(1)	2.297(4)
				2.868(1)
				<b>2.583</b>

The differences between the ordered and disordered models are explained in the text. Where necessary the average bond distances are given in bold.

here for the high-temperature cubic cryolite phase, although we note that the displacement parameters for the F remains somewhat higher in the Marx and Ibberson (19) model ( $3.6 \text{ \AA}^3$ ) than when the F is at the  $96k$  site ( $2.5 \text{ \AA}^3$ ).

### 3.3. Phase transition

Fig. 4 shows the temperature dependence of the lattice parameters for  $\text{Na}_3\text{AlF}_6$ . These results are consistent with the description of Steward and Rooksby in their earlier study [11]. The most striking feature is the sharp discontinuity near  $567^\circ\text{C}$  indicative of a first-order phase transition. Prior to this the nearly linear thermal expansion of the unit-cell lengths is unexceptional and

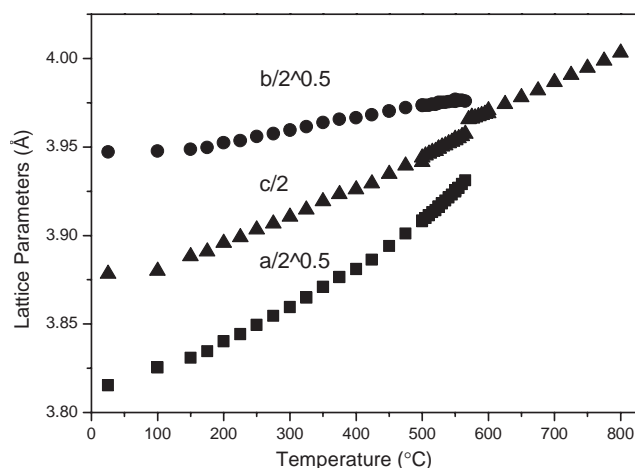


Fig. 4. Temperature dependence of the lattice parameters for  $\text{Na}_3\text{AlF}_6$  showing the presence of a first-order monoclinic to cubic phase transition near  $567^\circ\text{C}$ . In the monoclinic phase the cell parameters have been reduced to the equivalent perovskite values as follows:  $a = \sqrt{2}a_p$ ,  $b = \sqrt{2}a_p$  and  $c = 2a_p$ . In the cubic phase an equivalent reduction has been imposed  $a = 2a_p$ . In all cases ends of the cell parameters are smaller than the symbols.

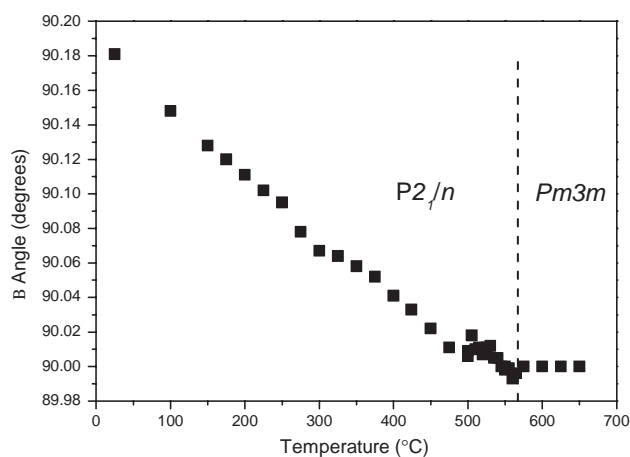


Fig. 5. Temperature dependence of the monoclinic beta angle as the temperature. The dashed vertical line shows the position of the first-order phase transition.

is good agreement with that found in earlier studies [11,12]. It is noteworthy that the monoclinic angle, which exhibits an almost linear decrease as the temperature is increased to  $500^\circ\text{C}$ , Fig. 5 becomes equal, within the precision of the present refinements to  $90^\circ$  near  $500^\circ\text{C}$ , some 50 or so degrees below the first-order phase transition. It is clear from Fig. 4 that the lattice parameters remain noticeably different so that the symmetry of the  $\text{Na}_3\text{AlF}_6$  is at least orthorhombic. Comparison of the profiles recorded at  $450^\circ\text{C}$  and  $550^\circ\text{C}$ , that is above and below the point at which the refined monoclinic angle becomes equal to  $90^\circ$  did not show the loss of any reflections and it was concluded that both the in-phase and out-of-phase tilts persist above  $550^\circ\text{C}$  and that the structure remains face centered.

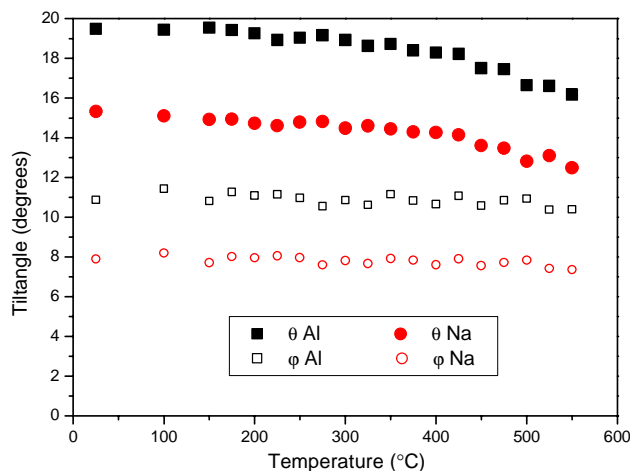


Fig. 6. Temperature dependence of the octahedra tilt angles for  $\text{Na}_3\text{AlF}_6$  calculated from the refined atomic coordinates. The tilt about the cubic, four-fold axis is given by  $\varphi$  and that about the two-fold axis by  $\theta$ .

We then considered the possibility of a continuous phase transition from the monoclinic  $P2_1/n$  structure to an orthorhombic phase as suggested by Yang [12]. Using group theory Howard and co-workers have recently identified possible sequences of phase transitions in double perovskites with rock-salt like ordering and by comparison with this work [20] we cannot identify any candidate phases. Yang [12] concluded that the  $Immm$  phases exists as a consequence of a simultaneous application of two modes,  $\Gamma_4^+$  and  $Y_2^+$  from low-temperature monoclinic  $P2_1/n$  phase. There is no simple distortion that would allow the transition from  $Immm$  to the parent cubic structure in  $Fm\bar{3}m$ . We believe our hypothesis of a direct first-order transition from  $P2_1/n$  to  $Fm\bar{3}m$  is the more reasonable. There are a number of examples in the perovskite literature where the diffraction patterns apparently indicate one metric cell, but the structure actually has lower symmetry [6,7,21]. This appears to be the case for  $\text{Na}_3\text{AlF}_6$  between  $500^\circ\text{C}$  and  $565^\circ\text{C}$ .

As indicated previously the monoclinic structure has an  $a^-b^-c^+$  tilting pattern and following Groen [22] the refined atomic co-ordinates have been used to calculate the magnitude of the tilts about the  $011$  ( $\varphi$ ) and  $110$  ( $\theta$ ) axis of the cubic aristotype. For simple  $\text{ABX}_3$  perovskites it has been found [5,7–10] that continuous transitions to a higher symmetry structure involve the progressive removal of one or more of the tilts. The temperature dependence of the tilts in  $\text{Na}_3\text{AlF}_6$  are illustrated in Fig. 6 and from these it is clear that a continuous transition to a higher symmetry structure is still somewhat distant. As described by Mitchell [1] the tilts of the smaller  $\text{AlF}_6$  octahedra are smaller than those of the larger  $\text{NaF}_6$  octahedra.

Consequently we believe that  $\text{Na}_3\text{AlF}_6$  remains monoclinic up to the point of the first order phase

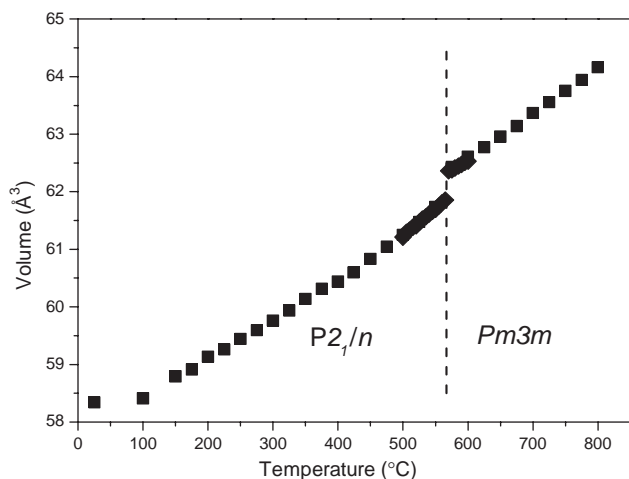


Fig. 7. Temperature dependence of the cell volume for  $\text{Na}_3\text{AlF}_6$  showing the presence of a first-order monoclinic to cubic phase transition near  $567^\circ\text{C}$ . For ease of comparison the volumes equivalent to that of the parent perovskite are plotted.

transition. As seen in Fig. 7 this phase transition is accompanied by a noticeable increase in the cell volume as the structure becomes cubic.

#### 4. Conclusion

We have demonstrated that very accurate and precise structures of the double perovskite,  $\text{Na}_3\text{AlF}_6$ , can be obtained using high-resolution synchrotron powder diffraction methods. The structure of this synthetic sample of cryolite has been found to be monoclinic from room temperature to  $560^\circ\text{C}$ . Just above this a first-order phase transition to a cubic structure is observed. The monoclinic phase is characterized by large in-phase and out-of-phase tilts of the  $\text{AlF}_6$  and  $\text{NaF}_6$  octahedra. As for the simple  $\text{ABX}_3$  perovskites these tilts in  $\text{Na}_3\text{AlF}_6$  are believed to be a consequence of the less than optimal size of the  $\text{Na}^+$  ions on the perovskite A-type site. Although the magnitude of these tilts is progressively reduced as the temperature is increased they remain relatively large over the entire temperature range. It can be concluded that any continuous phase transition involving a loss of tilting is still remote at  $565^\circ\text{C}$ . The high-temperature cubic phase is characterized by static displacive disorder of the F anions. The effect of this disorder on the local bond distances is similar to that of the tilts and is necessary to stabilize the cubic structure.

#### Acknowledgments

This work performed at the Australian National Beamline Facility was supported by the Australian Synchrotron Research Program, which is funded by the Commonwealth of Australia under the Major National Research Facilities program. BJK acknowledges the support of the Australian Research Council and numerous helpful discussions with Dr. C.J. Howard. The assistance of Dr. James Hester at the ANBF is gratefully acknowledged.

#### References

- [1] R.H. Mitchell, *Perovskites—Modern and Ancient*, Almaz Press, Thunder Bay, Ontario, 2002.
- [2] M.T. Anderson, K.B. Greenwood, G.A. Taylor, K.R. Poeppelmeier, *Prog. Solid State Chem.* 22 (1993) 197.
- [3] I.N. Flerov, M.V. Gorev, K.S. Aleksandrov, A. Tressaud, A. Grannec, M. Couzi, *Mater. Sci. Eng. R* 24 (1998) 81.
- [4] C.J. Howard, H.T. Stokes, *Acta Crystallogr. B* 54 (1998) 782; C.J. Howard, H.T. Stokes, *Acta Crystallogr. erratum B* 58 (2002) 565.
- [5] Y. Zhao, D.J. Weidner, J.B. Parise, D.E. Cox, *Phys. Earth. Planet Interiors* 76 (1993) 17.
- [6] B.J. Kennedy, C.J. Howard, B.C. Chakoumakos, *J. Phys. C: Condens. Matter* 11 (1999) 479.
- [7] C.J. Howard, K.S. Knight, B.J. Kennedy, E.H. Kisi, *J. Phys.: Condens. Matter* 12 (2000) L677.
- [8] B.J. Kennedy, B.A. Hunter, J.R. Hester, *Phys. Rev. B* 65 (2002) 224103.
- [9] B.J. Kennedy, A.K. Prodjosantoso, C.J. Howard, *J. Phys. C: Condens. Matter* 11 (1999) 6319.
- [10] B.J. Kennedy, C.J. Howard, G.J. Thorogood, J.R. Hester, *J. Solid State Chem.* 161 (2001) 106.
- [11] E.G. Steward, H. Rooksby, *Acta Crystallogr.* 6 (1953) 49.
- [12] H. Yang, S. Ghose, D. Hatch, *Phys. Chem. Minerals* 19 (1993) 528.
- [13] T.M. Sabine, B.J. Kennedy, R.F. Garrett, G.J. Foran, D.J. Cookson, *J. Appl. Crystallogr.* 28 (1995) 513.
- [14] C.J. Howard, B.A. Hunter, *A computer program for Rietveld analysis of X-ray and neutron powder diffraction patterns*, Lucas Heights Research Laboratories, NSW, Australia, 1998, pp. 1–27.
- [15] F.C. Hawthorne, R.B. Ferguson, *Canad. Mineral* 13 (1975) 377.
- [16] A.M. Glazer, *Acta Crystallogr. B* 28 (1972) 3384; A.M. Glazer, *Acta Crystallogr. A* 31 (1975) 756.
- [17] K.C. Ross, R.H. Mitchell, A.R. Chakhmouradian, *J. Solid State Chem.* 172 (2003) 95.
- [18] D.L. Corker, A.M. Glazer, J. Dec, K. Roleder, R.W. Whatmore, *Acta Crystallogr. B* 53 (1997) 135.
- [19] R. Mark, R.M. Ibberson, *J. Alloys Compd.* 261 (1997) 123.
- [20] C.J. Howard, B.J. Kennedy, P.W. Woodward, *Acta Crystallogr. B* 59 (2003) 463.
- [21] C.J. Howard, R.L. Withers, B.J. Kennedy, *J. Solid State Chem.* 160 (2001) 8.
- [22] W.A. Groen, F.P.F. Van Berkel, D.J.W. Ijdo, *Acta Crystallogr. C* 42 (1986) 1472.